European Geothermal Congress 2016
Strasbourg, France, 19-24 Sept 2016

# Modelling focal mechanism errors of seismicity induced at Rittershoffen geothermal field (Alsace, France)

X. Kinnaert[1,2*], E. Gaucher[1], T. Kohl[1] and U. Achauer[2]

[1] Karlsruhe Institute of Technology, Institute of Applied Geosciences, Geothermal Research, Karlsruhe, Germany

[2] EOST-IPGS UMR7516, Strasbourg, France

xavier.kinnaert@kit.edu

**Keywords:** EGS, fault plane, inaccuracy, uncertainty, velocity model error

## ABSTRACT

The determination of focal mechanisms of earthquakes induced in geothermal fields is of primary interest for reservoir characterization. For example, parameters like fault identification, faulting regime and stress field may be derived from it. The impact of a few parameters on the earthquake focal-mechanism determination is investigated using a three-step approach. First, synthetic waveforms are created for double-couple sources whose strike, dip and rake are consistent with the fault plane on which they are located. From the synthetic waveforms generated on the network, the polarity of P-waves and the amplitudes of P- and S-waves are measured to constitute the observed data. In the second step, the polarities and amplitude ratios are inverted to compute the focal mechanisms, once the earthquake was located. However, to represent the lack of knowledge or simplifications, the initial velocity model is replaced for this inversion. In the last step, the focal mechanisms obtained are compared with the original ones.

The method is applied to the deep geothermal site of Rittershoffen (France). In 2013, a massive water injection was performed at approximately 2.5 km depth to enhance the GRT1 well productivity. Induced seismicity was recorded by a surface network installed in several steps. After discussing the capabilities of the seismic network to estimate the focal mechanisms in a perfect case, we investigate the impact of approximating a 3D velocity model including a fault and a shifted block by a 1D velocity model. For each case, results using only polarities or polarities and amplitude ratios are compared.

The angular inaccuracies associated with the slip vector determination are usually smaller than the corresponding uncertainties or of the same order. The addition of amplitude ratios data only affect the focal mechanism of sources located in a low velocity zone and the impact of an incorrect velocity model can only be seen on focal mechanism uncertainties.

## 1. INTRODUCTION

In geothermal applications, the determination of focal mechanisms (FMs) of natural or induced earthquakes is of primary interest. This parameter may be used to identify and characterize active faults and fractures of the reservoir, and to build fracture networks (Koepke *et al.*). It is also of major interest for geomechanical interpretation and stress-field analysis (Schoenball *et al.* 2014). The FM is a secondary attribute of an earthquake in the sense that it is usually determined once the earthquake hypocentre (the first attribute) has been located. Accordingly, FM determination is neither independent from the earthquake location nor from the errors in location. Hence, quantifying the error associated with the determination of FM is of interest to properly interpret the associated results..

The earthquake FM error can be described as the combination of the FM inaccuracy and the FM uncertainty. The FM uncertainties are directly linked to the uncertainties which are taken into account during the inversion process (Tarantola 2005). Typically, *a priori* take-off angle or polarity uncertainties contribute to *a posteriori* FM uncertainties (Hardebeck and Shearer 2002). On the other hand FM inaccuracies are commonly due to the lack of knowledge of the sub-surface or its simplification. For example, a bad location of the earthquake or/and a wrong velocity model would induce a wrong take-off angle which would lead to an incorrect slip vector (Hardebeck and Shearer 2003). The quantification of FM uncertainties is nowadays common and several software can provide them (e.g. Hardebeck and Shearer; Snoke 2003). On the contrary, the quantification of the FM inaccuracy requires a special procedure.

This work focuses on the quantification of FM inaccuracies and uncertainties of earthquakes in the context of the Rittershoffen (France) deep geothermal field. It follows the study of Kinnaert *et al.* (2016) performed on the same site and dedicated to the quantification of errors of earthquake absolute location at this site. This work investigates the impact of velocity model errors on the FM inaccuracies and uncertainties as well as their relationship with the seismic monitoring network design.

## 2. METHODOLGY

To quantify the seismic event FM uncertainties and inaccuracies, a three-step method is applied. During the synthetic modelling step, seismic waveforms are created at the position of different seismic sensors for sources distributed on a plane and for a fixed double-couple FM. In this step, the assumptions are supposed to represent the reality of the sub-surface. The waveform are computed using the finite-difference method of Virieux (1984; 1986) implemented in the SOFI3D software (Bohlen 2002). Then, the polarities of the P-wave are determined directly from the waveforms associated with the vertical component of the sensors. On 3C-sensors, P- and S-wave amplitudes are determined in a window around the arrival as the maximum 3D-amplitude. The 3D-amplitude is defined as the square root of the sum of the squares of the amplitudes recorded by each component of the sensor. In the second step, the polarities and amplitude ratios obtained are considered as observations and are used to (re-)compute the FM of the synthetic seismic events. Nevertheless, the velocity model is changed compared to the model used during the synthetic modelling step, and different seismic network designs are also used. The FM determination is carried out by the HASH software (Hardebeck and Shearer 2002, 2003) which uses a grid-search method over the strike, dip and rake angles defining the FM from modelled azimuth and take-off angles at the source focus. These later are obtained from the NonLinLoc package (Lomax 2011), which is also used to relocate the earthquake in the changed velocity model (Kinnaert *et al.* 2016). The HASH software has the advantage to provide uncertainties associated with the FM and to handle FM determination with or without observation of amplitude ratios. The uncertainties are given as two angles deviating from the slip vectors of the obtained fault plane and auxiliary plane of the best FM. The maximum angle is considered as the uncertainty. In the third and last step, the slip vectors of the obtained FMs are compared with those of the initial FM. The angle differences between the initial slip vectors and the computed ones (for the best FM) is calculated, and minimum difference is taken as the inaccuracy for each acceptable FM.

## 3. THE RITTERSHOFFEN GEOTHERMAL SITE

### 3.1. Geological settings

The Rittershoffen geothermal site is located in the Upper Rhine Graben (URG), in France. The geological and structural settings of the shallow sub-surface in the URG are well known due to earlier investigations from the oil industry (Schnaebele 1948). Seismic profiles provided good knowledge of the sedimentary cover in the Rittershoffen area and highlighted numerous horst and grabens structures (Wentzel and Brun 1991). The presence of fracture networks in the sub-surface and of thermal anomalies (Bailleux *et al.* 2013) makes the URG a suitable place for geothermal development.

At Rittershoffen, the reservoir was developed at ~2500 m depth, at the interface between tertiary sediment layers and the granitic basement. The site benefits from one of the highest temperature gradient in the URG and the temperature reaches ~165°C at 1800 m depth (Baujard *et al.* 2014). A major normal fault peculiar to the Rittershoffen geological structure was targeted by the two wells constituting the doublet. In the well GRT1, this fault is observed at a depth of ~2.4 km, 200 m deeper than the sediment/granite interface. The fault is oriented nearly NS, dips 60°W, and account for a vertical shift of 200 m.

### 3.2. Seismicity induced by GRT1 stimulation

In 2013, the well GRT1 was stimulated many times and induced several hundredths of unfelt micro-earthquakes all with local magnitude $M_l < 1.6$ (Maurer *et al.* 2015). The seismicity was recorded by surface seismic stations. It is located along a N-S to NNE-SSW direction within a zone extending 2 km to the north, 1 km to the east and 2 km in depth (Maurer *et al.* 2015), and centred in the proximity of GRT1 bottom hole. The expected location errors for this seismic cloud were investigated using synthetic locations (Kinnaert *et al.* 2016) .

### 3.3. Velocity models

#### *3.3.1 1D velocity model*

A 1D velocity profile was derived from different data measured in the well GRT1 at Rittershoffen (Figure 1). This model was used to process the induced seismicity and its errors (Maurer *et al.* 2015; Kinnaert *et al.* 2016). It will be considered here as the reference velocity model. In this layered model, the P-wave velocity ranges between 1320 $m.s^{-1}$ and 5815 $m.s^{-1}$, the S-wave velocity varies between 620 $m.s^{-1}$ and 3275 $m.s^{-1}$. The Vp/Vs ratio varies between 1.68 and 2.12. The profile presents three embedded low-velocity layers and two large velocity contrasts (at 1365 m and 2200 m corresponding to the Lias layer and the top of the granite respectively).

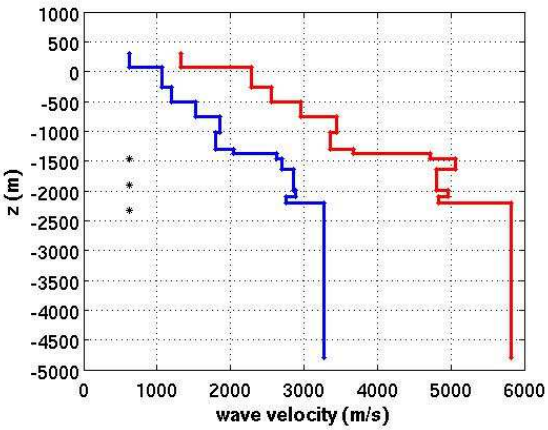


**Figure 1: P- (red) and S- (blue) reference velocity profiles. The black stars indicate the depths of the synthetic sources.**

#### *3.3.1 3D velocity model*

The major fault at Rittershoffen was targeted by the two wells of the geothermal doublet. It is oriented NS and is dipping 60° to the west. This is also a normal fault which exhibit 200 m vertical shift. Accordingly, we build a 3D-velocity model which consists in shifting the 1D-velocity profile along the fault. Hence, in the eastern block, the average velocity is higher than on the western block. This 3D model will be used as representative of the true Earth and was used in previous studies (Gaucher *et al.* 2016; Kinnaert *et al.* 2016).

### 3.4. Seismic monitoring networks

The earthquakes induced by the stimulation of the well GRT1 were recorded by 12 permanent and 5 temporary stations (Maurer *et al.* 2015) (Figure 2). The 5 temporary stations have 3C-sensors and a sampling rate of 300 Hz. Among the permanent stations, sampling at 100 or 150 Hz, 7 have 3C-sensors whereas the others have only a vertical sensor. Among them, 2 stations were not used because the signal-to-noise ratio was too low to allow picking (N. Cuenot private communication, 2015). This network is called Net15 is the following. To increase the seismic network coverage, 24 temporary stations were installed before the drilling of the well GRT2. Their characteristics are similar to those of the 5 temporary sensors previously described. This larger network is called Net41 in the following.

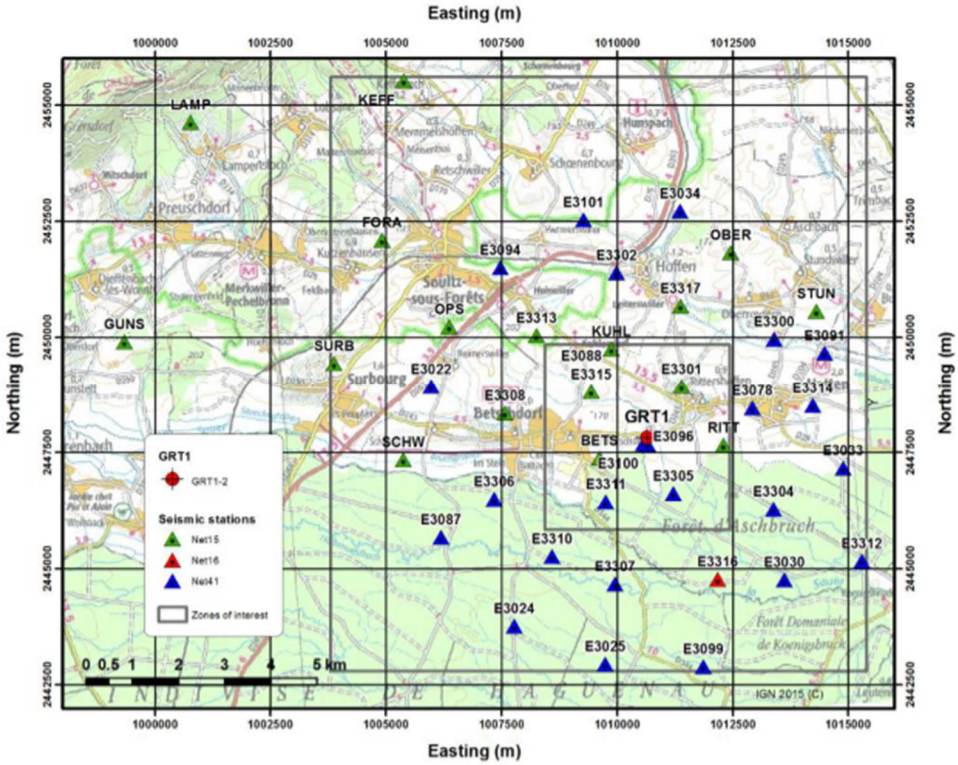


**Figure 2: Geometry of the seismic networks monitoring seismicity at Rittershoffen geothermal field. The Net15 seismic network (green triangles) monitored the stimulations of GRT1 well in 2013. The Net16 network contains all stations from Net15 and an additional temporary station, E3316 (red triangle). The whole Net41 seismic network was installed before the drilling of GRT2 in 2014 and consists of the Net16 with the additional stations represented by blue triangles. The GRT1 well-head (red crossed circle), is also displayed. All coordinates are given in Lambert II extended system.**

### 3.5. Synthetic event hypocentres

To investigate the FM errors, nine hypocentres were simulated on the fault plane which crosses the GRT1 well at 2089 m depth. Three by three sources are regularly distributed every 500 m in the north-south and along dip directions of the plane. Hence, the central source is located at the well and on the fault. With regards to the velocity model, the three deeper sources are located in the granite, the three intermediate sources in the low Vp velocity zone in the sediments, and the shallower sources close to the shallower high velocity contrast (Figure 1).

## 4. RESULTS AND DISCUSSION

### 4.1. Reliability of the methodology

To test the methodology, we computed the FM of the central source using the denser seismic monitoring network, Net41, which has a good azimuthal coverage (see Figure 2), first in a homogeneous velocity model and in the reference 1D velocity model (Figure 3).

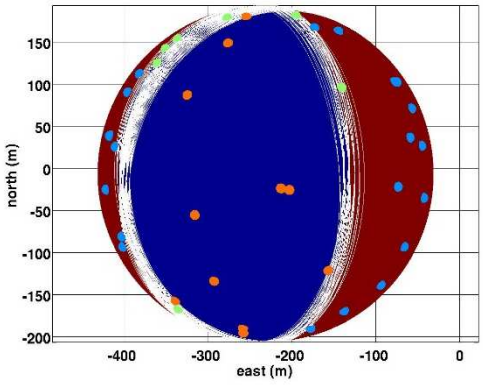


**Figure 3: Upper view of the beachball of the best focal mechanism for the central source. Solution obtained in the 1D reference velocity model, from P-wave polarities on Net41. The white lines show all acceptable FMs. The circles show the polarities observed at the different seismic stations according to their azimuth and take-off angles: green for undetermined, blue for positive, orange for negative.**

Neither in the homogeneous model nor in the reference 1D model do the inaccuracies exceed 12° from the expected normal faulting FM (180° strike, 60° dip, -90° rake). An inaccuracy of ~3° is obtained for the best FM. The obtained uncertainty is around 6°. These results are the same considering the use of the polarities only or the polarities and amplitude ratios.

These tests prove the reliability of the proposed method which was then used for more complex studies.

### 4.2. Network effect in 3D velocity model

We investigate the effect of the lay-out of the seismic network which was monitoring the GRT1 stimulation, Net15, on the retrieval of the original FMs. This is of specific interest because there is a seismic coverage gap south of the well. To do so, we invert the FM in the 3D velocity model, which was also used to create the synthetic waveforms. Hence, the synthetic source location and take-off angle calculations were done in the 3D model. This study provides the minimal FM errors which can be obtained at Rittershoffen during GRT1 stimulation.

Figure 4 shows the angular inaccuracy of the normal vectors of all acceptable FMs compared to the normal vector of the original FM as well as the angular inaccuracy of the mean normal vector.

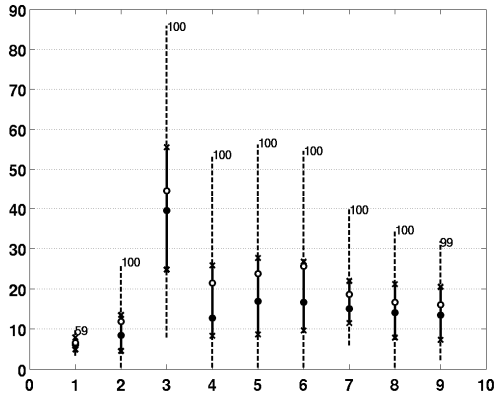


**Figure 4: Boxplot representation (Tukey 1977) of the angular inaccuracy (in degrees) of the normal vector of the acceptable focal mechanisms obtained using P-wave polarities measured on Net15. Each boxplot shows the inaccuracies for one source. The first three correspond to the shallowest sources and the last three to the deepest ones. For each triplet, the northern source is shown first. Each boxplot shows the median (full disk), the first and third quartiles (crosses) and the range (dashed line) of the angular discrepancies between both fault plan normals. The angular inaccuracy for the mean normal vector is shown by the unfilled disk and the number of FMs used to perform the statistics is written above each boxplot.**

The angular inaccuracy of the mean vector varies between 5 and 45° (Figure 4). Apart from the shallowest-southern and the deepest-northern sources, the original solution always belongs to the range of possible solutions. Except for the shallowest-southern source, which shows the highest mean vector inaccuracy, 45°, all other sources have mean vector within ~25° from the original one. It seems that inaccuracies for the southern sources decrease with depth in values and in range. From ~45° for the shallowest source, the mean vector inaccuracy decreases to less than 30° at intermediate depth and to less than 20° for the deepest source. The maximum inaccuracy decreases from ~85° to ~35°. Apart from

the shallowest-southern source, it looks like the angular inaccuracies are smaller for the deepest and the shallowest sources than for sources at intermediate depth.

One also have to mention that the inaccuracy associated with the mean normal vector usually do not fit with the median of the inaccuracies, the latter being always smaller. This means that the set of acceptable FMs are not equally distributed around that corresponding to the mean vector.

On the other hand, the inaccuracies associated with the strike, and dip angles defining the fault plane were studied separately for each acceptable FM of each source (Figure 5).

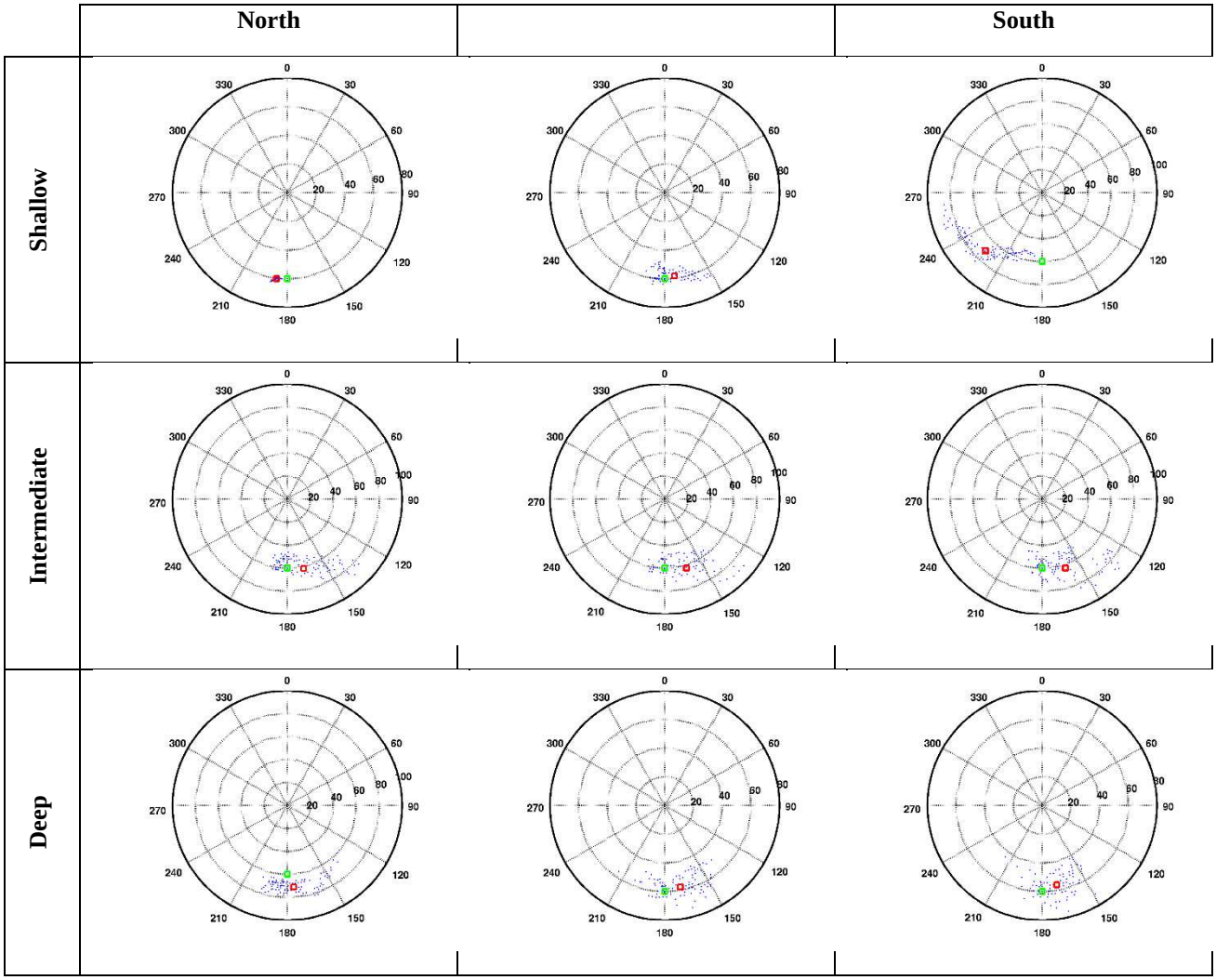


**Figure 5: Polar representation of strike and dip angles for all acceptable FMs. The mean and the original fault planes solutions are represented by the red and green squares respectively. Rows of the table correspond to source depth whereas columns correspond to source latitude (north-left, south-right).**

For seven cases over nine, the mean vector from all acceptable FMs and the vector associated with the original FM, the azimuthal inaccuracy is negative. The two exceptions are the northern and southern shallowest sources. This strike inaccuracy is usually in the range [-45°, 30°] with the major part of acceptable FMs in the interval [-30°, 15°]. Nevertheless, the set of acceptable strikes vary according to the source location. However, no spatial and regular variation of the dip discrepancies as a function of the source location seems to appear.

To conclude, with the Net15, the same original fault plane could be interpreted as multiple plane solutions depending on the source location, if the focal mechanisms inaccuracies and uncertainties are not taken into account, and even in a correct velocity model.

### 4.3. Effect of wrong velocity model

As shown by Kinnaert *et al.* (2016), locating in the 1D velocity model instead of locating in the 3D fault model (assuming the latter is representative of the true Earth) may lead to location inaccuracies up to 300-400

m. Here, we investigate the further impact these assumptions could bring into the FM determination.

For the modelling step, the 3D velocity model was taken as the reference and the waveforms and arrival times computed in it. Then, in the inversion step, the 1D velocity model was used first to relocate the sources, as proposed by Kinnaert *et al.* (2016), and to compute the azimuth and take-off angles from the computed hypocentre. Hence, the waveforms represent the reality of the sub-surface whereas the source locations and the emergence angles at the sources account for the bias introduced in the inverse problem.

The results on angular inaccuracies are shown in Figure 6, for the case where only the P-wave polarities were used, and the focal mechanism obtained for the central source is represented in Figure 7, for the case where both the P-wave polarities and the amplitude ratios were used.

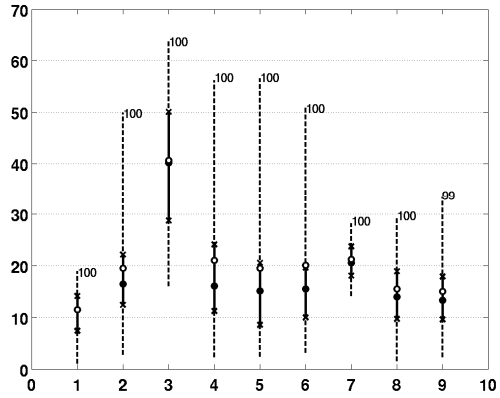


**Figure 6: Angular inaccuracy (in degree) of the normals to the acceptable fault plane solutions, which were determined by the P-wave polarities measured on Net15 in the 3D to 1D velocity model. See Figure 4 for symbol details.**

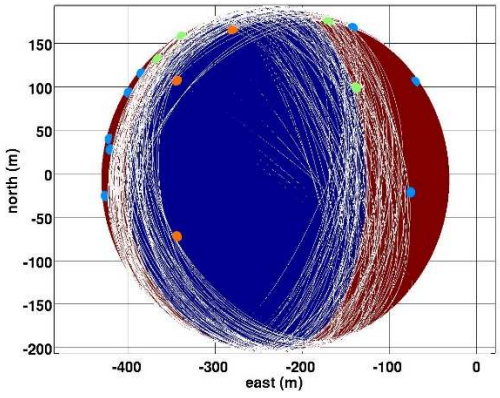


**Figure 7: Upper view of the beachball of the best focal mechanism for the central source. Solution determined by the P-wave polarities and amplitude ratios measured on Net15 in the 3D to 1D velocity model. Same representation as in Figure 3.**

The angular inaccuracies are not very different from the inaccuracies observed in the previous 3D model perfect case (Figure 6 vs Figure 4). One can however notice that the original fault plane is no more in the range of the possible solutions, for all considered sources. Furthermore, the inaccuracies of the two shallowest-northern sources are increased by about 5°.

## 5. CONCLUSION

In this paper, we mainly focused on the development of a technique to quantify focal mechanism uncertainties and inaccuracies at a geothermal reservoir scale. This technique was firstly validated on simple cases and then applied on a real case to study the impact of a velocity model simplification on focal mechanism determination.

Hence, it was shown that, at Rittershoffen geothermal field, the determination of the focal mechanisms for the seismicity induced during the GRT1 stimulation, may be inaccurate, in average, by 5° to 45° with uncertainties of around 5° to 30° if polarities are used and with uncertainties up to 40° when polarities and amplitude ratios are used. These effects are resulting from the finite coverage of the monitoring network only. In addition, assuming a 1D velocity model instead of the 3D fault model can lead to inaccuracies between 10° and 40° for the mean focal mechanism and uncertainties between 10° and 35°. These results suggest that, with the network monitoring during the GRT1 stimulation, multiple sources located on the same original fault plane could be interpreted as belonging to different ones according to their determined FMs, especially if the focal mechanisms inaccuracies and uncertainties are not taken into account, and even in a correct velocity model.

## REFERENCES

Bailleux P., Schill E., Edel J.-B. and Mauri G. 2013. Localization of temperature anomalies in the Upper Rhine Graben: insights from geophysics and neotectonic activity. *International Geology Review* **55**.

Baujard C., Villadangos G., Genter A., Graff J.-J., Schmittbuhl J. and Maurer V. 2014. The ECOGI geothermal project in the framework of a regional development of geothermal energy in the Upper Rhine Valley, 74th annual meeting of the German Geophysical Society (DGG), Karlsruhe, 10-13 March.

Bohlen T. 2002. Parallel 3-D viscoelastic finite difference seismic modelling. *Computers & Geosciences* **28** (8), 887–899.

Gaucher E., Kinnaert X., Achauer U. and Kohl T. (eds.). 2016. *Propagation of Velocity Model Errors in Earthquake Absolute Locations: Application to the Rittershoffen Geothermal Field*, 41st Workshop on Geothermal Reservoir Engineering, Stanford University, Stanford.

Hardebeck J.L. and Shearer P.M. HASH: A FORTRAN Program for Computing Earthquake First-Motion Focal Mechanisms-v1.2-January 31, 2008.

Hardebeck J.L. and Shearer P.M. 2002. A New Method for Determining First-Motion Focal Mechanisms. *Bulletin of the Seismological Society of America* **92** (6), 2264–2276.

Hardebeck J.L. and Shearer P.M. 2003. Using S/P Amplitude Ratios to Constrain the Focal Mechanisms of Small Earthquakes. *Bulletin of the Seismological Society of America* **93** (6), 2434–2444.

Kinnaert X., Gaucher E., Achauer U. and Kohl T. 2016. Modelling earthquake location errors at a reservoir scale: a case study in the Upper Rhine Graben. *Geophysical Journal International* **206** (2), 861–879.

Koepke R., Gaucher E., Meixner J. and Kohl T. A method to interpret induced seismicity clouds as a fracture network. In: *EGC 2016, 19-23 septembre, Strasbourg*.

Lomax A. 2011. *NonLinLoc: Probabilistic, Non-Linear, Global-Search Earthquake Location in 3D media.* ALomax Scientific.

Maurer V., Cuenot N., Gaucher E., Grunberg M., Vergne J., Wodling H., Lehujeru M. and Schmittbuhl J. 2015. Seismic monitoring of the Rittershoffen EGS project (Alsace, France): World Geothermal Congress.

Schnaebele R. 1948. *Monographie géologique du champ pétrolifère de Pechelbronn*. Mémoire du Service de la Carte Géologique d'Alsace et de Lorraine.

Schoenball M., Dorbath L., Gaucher E., Wellmann J.F. and Kohl T. 2014. Change of stress regime during geothermal reservoir stimulation. *Geophysical Research Letters* **41** (4), 1163–1170.

Snoke J.A. 2003. FOCMEC: focal mechanism determinations. *International Handbook of Earthquake and Engineering Seismology* **85**.

Tarantola A. (ed.). 2005. *Inverse problem theory and methods for model parameter estimation.* Society for Industrial and Applied Mathematics.

Tukey J.W. 1977. *Exploratory Data Analysis.* Addison-Wesley. ISBN 0201076160.

Virieux J. 1984. SH-wave propagation in heterogeneous media: Velocity-stress finite-difference method. *GEOPHYSICS* **49** (11), 1933–1942.

Virieux J. 1986. P-SV wave propagation in heterogeneous media: Velocity-stress finite-difference method. *GEOPHYSICS* **51** (4), 889–901.

Wentzel F. and Brun J.-P. 1991. A deep Reflection Seismic Line across theNorthern Rhine Graben. *Earth and Planetary Science Letters* **104**, 140–150.

**Acknowledgment**

This work was conducted in the framework of the excellence laboratory “Labex G-EAU-THERMIE PROFONDE” (University of Strasbourg). It was funded by the French National Research Agency, as part of the French “Investments for the future” program, by the Energie Baden-Württemberg AG (EnBW), the French institution CNRS, and by the French-German University (DFH-UFA).